

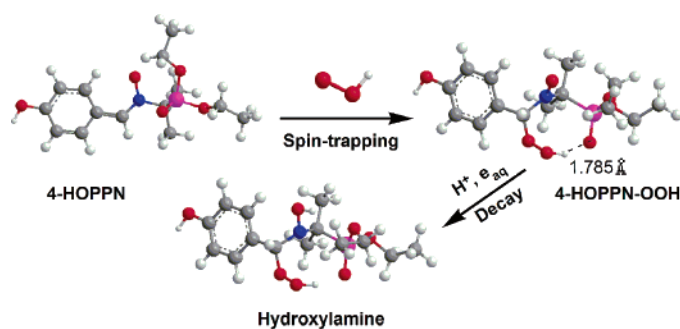
Effect of the Phosphoryl Substituent in the Linear Nitron on the Spin Trapping of Superoxide Radical and the Stability of the Superoxide Adduct: Combined Experimental and Theoretical Studies

Yang-Ping Liu,^{†,‡} Lan-Fen Wang,^{†,‡} Zhou Nie,[†] Yi-Qiong Ji,[†] Yang Liu,^{*,†}
Ke-Jian Liu,^{*,§} and Qiu Tian[†]

State Key Laboratory for Structural Chemistry of Unstable and Stable Species, Center for Molecular Science, Institute of Chemistry, Chinese Academy of Sciences, Beijing 100080, China, Graduate School, The Chinese Academy of Sciences, Beijing 100080, China, and College of Pharmacy, University of New Mexico, 2502 Marble NE, Albuquerque, New Mexico 87131

yliu@iccas.ac.cn; jliu@unm.edu

Received June 12, 2006



A new phosphorylated linear nitron *N*-(4-hydroxybenzylidene)-1-diethoxyphosphoryl-1-methylethylamine *N*-oxide (4-HOPPN) was synthesized, and its X-ray structure was determined. The spin trapping ability of various kinds of free radicals by 4-HOPPN was evaluated. Kinetic study of decay of the superoxide spin adduct (4-HOPPN-OOH) shows the half-life time of 8.8 min. On the basis of the X-ray structural coordinates, theoretical analyses using density functional theory (DFT) calculations at the B3LYP/6-31+G(d,p)//B3LYP/6-31G(d) level were performed on spin-trapping reactions of superoxide radical with 4-HOPPN and PBN and three possible decay routes for their corresponding superoxide adducts. The comparative calculations on the spin-trapping reactions with superoxide radical predicted that both spin traps share an identical reaction type and have comparable potency when spin trapping superoxide radical. Analysis of the optimized geometries of 4-HOPPN-OOH and PBN-OOH reveals that an introduction of the phosphoryl group can efficiently stabilize the spin adduct through the intramolecular H-bonds, the intramolecular nonbonding attractive interactions, as well as the bulky steric protection. Examination of the decomposition thermodynamics of 4-HOPPN-OOH and PBN-OOH further supports the stabilizing role of the phosphoryl group to a linear phosphorylated spin adduct.

Introduction

Spin trapping as a valuable technique for detection of transient radicals has been extensively utilized to investigate radical

processes involved in chemical or biochemical environments. In general, nitron reacts with transient radical resulting in the stable nitroxide radical that is detected by electron spin resonance (ESR). Of all the available nitrones, α -phenyl-*N*-*tert*-butylnitron (PBN) and 5,5-dimethyl-1-pyrroline *N*-oxide (DMPO) as representatives of the linear and cyclic nitrones, respectively, have received the most attention. However, their uses are limited due to the low stability of their superoxide spin adducts. The

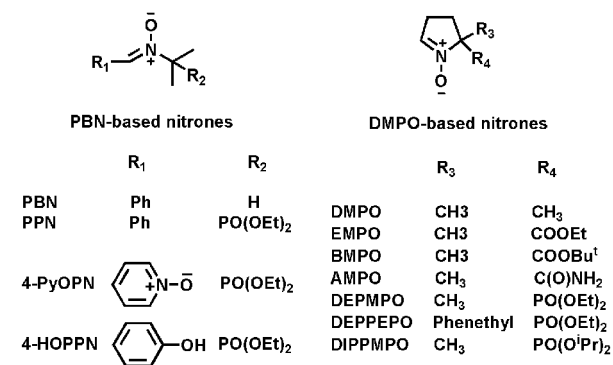
* To whom correspondence should be addressed. (Y.L.) Tel: +86 10 62571074. Fax: +86 10 62559373. (K.-J.L.) Tel: (505) 272-9546. Fax: (505) 272-6749.

[†] Chinese Academy of Sciences.

[‡] Both authors contributed equally to this work.

[§] University of New Mexico.

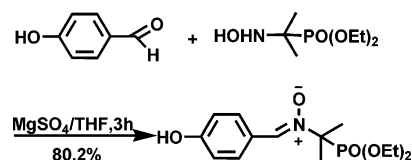
CHART 1



half-life time of DMPO-OOH was under a minute at room temperature,¹ while that of PBN-OOH was even shorter.²

Considering that superoxide radical is a primary upstream radical of the radical reaction chain inducing oxidative stress³ and is involved in a number of signal transduction pathways,⁴ many efforts have been devoted to developing new spin traps for superoxide radical and structurally diverse nitrones have been synthesized.⁵ Among them, 5-diethoxyphosphoryl-5-methyl-1-pyrroline *N*-oxide (DEPMPO), one β -phosphorylated cyclic nitron, appears to be one of the most promising spin traps for superoxide radical and other reactive oxygen species (ROS) because of the considerably increased stability of its superoxide spin adduct (DEPMPO-OOH, half-life time $t_{1/2} \sim 14$ min).^{5a,6} Because of this, DEPMPO has been widely used in a variety of biological systems.⁷ Moreover, for the purpose of obtaining the lipophilic spin trap for ROS, the phosphoryl group was also introduced into the β position of PBN to create a linear nitron, such as 4-PyOPN or PPN (Chart 1).^{5d,8} The experimental results showed that these traps possess better properties of spin trapping superoxide radical as compared with their nonphosphorylated analogues. For example, relative to PBN, the phosphorylated linear nitrones *N*-benzylidene-1-diethoxyphosphoryl-1-methylethylamine *N*-oxide (PPN) and 1-diethoxyphosphoryl-1-methyl-*N*[(1-oxidopyridin-1-ium-4-yl)methylidene] ethylamine *N*-oxide (4-PyOPN) exhibited considerable improvements in the detec-

SCHEME 1. Synthesis of 4-HOPPN



tion of superoxide radical (the half-life times of the adducts: 6 and 7 min, respectively).^{5d,8} Therefore, it is of significant importance to investigate the exact reason the β -phosphorylated spin traps can enhance the efficiency of spin trapping of superoxide radical, since this knowledge can open up the possibilities of developing more efficient spin traps for superoxide radical.

In a previous study,⁹ we reported the first X-ray structure of the phosphorylated cyclic nitron, 5-diethoxyphosphoryl-5-phenethyl-1-pyrroline *N*-oxide (DEPPEPO). Thereafter, the X-ray structures of other cyclic nitrones such as 5-diisopropoxyphosphoryl-5-methyl-1-pyrroline *N*-oxide (DIPPMPPO),¹⁰ 5-carbamoyl-5-methyl-1-pyrroline *N*-oxide (AMPO),¹¹ and 5-butoxycarbonyl-5-methyl-1-pyrroline *N*-oxide (BMPO)¹² were also experimentally determined. Using these X-ray structural coordinates as the initial input data to program, a series of theoretical calculations^{11–13} have recently been performed to reasonably interpret the spin trapping properties of the cyclic nitrones containing various substituents. The theoretical calculation has shown potential for designing better cyclic spin traps,¹² but little theoretical attention has been paid to the β -phosphorylated linear nitrones.

Herein, in the light of spin-trapping ESR behaviors and X-ray structural coordination of a new phosphorylated linear nitron, [N-(4-hydroxybenzylidene)-1-diethoxyphosphoryl-1-methylethylamine *N*-oxide (4-HOPPN), and those from PBN, two possible routes for spin trapping of superoxide radical by 4-HOPPN and PBN as well as three proper mechanisms for explaining the decay of their superoxide spin adducts have been comparatively investigated from the theoretical views. In addition, spin trapping of various reactive radicals by 4-HOPPN was experimentally evaluated.

Results and Discussion

Experimental Analysis. Synthesis. As shown in Scheme 1, condensation of 4-hydroxybenzaldehyde on diethyl (1-hydroxyamino-1-methylethyl) phosphonate¹⁴ led to 4-HOPPN, and then the product was recrystallized in a mixture of *n*-hexane and ethyl acetate after purification by column chromatography.

X-ray Structure. It is valuable to explore the X-ray structure of 4-HOPPN since this experimental data can provide substantial

(1) Buettner, G. R.; Oberley, L. W. *Biochim. Biophys. Res. Commun.* **1978**, *83*, 69.

(2) Thomas, C. E.; Ohlweiler, D. F.; Carr, A. A.; Nieduzak, T. R.; Hay, D. A.; Adams, G.; Vaz, R.; Bernotas, R. C. *J. Biol. Chem.* **1996**, *271*, 3097.

(3) (a) Halliwell, B. *Am. J. Med.* **1991**, *91* (3C), 14S. (b) Halliwell, B.; Gutteridge, J. M. C. *Am. J. Med.* **1984**, *219*, 1. (c) Halliwell, B.; Chirico, S.; *Am. J. Clin. Nutr.* **1993**, *57* (S), 715S.

(4) (a) Finkel, T. *J. Leukocyte Biol.* **1999**, *65*, 337. (b) Wolin, M. S. *Arterioscler. Thromb. Vasc. Biol.* **2000**, *20*, 1430. (c) Droge, W. *Physiol. Rev.* **2002**, *82*, 47.

(5) (a) Fréjaville, C.; Karoui, H.; Tuccio, B.; Le Moigne, F.; Culcasi, M.; Pietri, S.; Lauricella, R.; Tordo, P. *J. Chem. Soc., Chem. Commun.* **1994**, 1793. (b) Olive, G.; Mercier, A.; Le Moigne, F.; Rockenbauer, A.; Tordo, P. *Free Radic. Biol. Med.* **2000**, *8*, 403. (c) Zhao, H.; Joseph, J.; Karoui, H.; Kalyanaram, B. *Free Radic. Biol. Med.* **2001**, *31*, 599. (d) Zeghdaoui, A.; Tuccio, B.; Finet, J. P.; Cerri, V.; Tordo, P. *J. Chem. Soc., Perkin Trans. 2* **1995**, 2087.

(6) Fréjaville, C.; Karoui, H.; Tuccio, B.; Le Moigne, F.; Culcasi, M.; Pietri, S.; Lauricella, R.; Tordo, P. *J. Med. Chem.* **1995**, *38*, 258.

(7) (a) Shi, H.; Timmins, G.; Monske, M.; Burdick, A.; Kalyanaram, B.; Liu, Y.; Clément, J. L.; Burchiel, S.; Liu, K. *J. Arch. Biochem. Biophys.* **2005**, *437*, 59. (b) Liu, K.; Sun, J.; Song, Y. G.; Liu, B.; Xu, Y. K.; Zhang, S. X.; Tian, Q.; Liu, Y. *Photosyn. Res.* **2004**, *81*, 41. (c) Vasquez-Vivar, J.; Kalyanaram, B.; Martasek, P.; Hogg, N.; Masters, B. S. S.; Karoui, H.; Tordo, P.; Pritchard, K. A. *Proc. Natl. Acad. Sci. U.S.A.* **1998**, *95*, 9220.

(8) (a) Tuccio, B.; Zeghdaoui, A.; Finet, J. P.; Cerri, V.; Tordo, P. *Res. Chem. Intermed.* **1996**, *22*, 393. (b) Roubaud, V.; Lauricella, R.; Tuccio, B.; Bouteiller, J. C.; Tordo, P. *Res. Chem. Intermed.* **1996**, *22*, 405.

(9) Xu, Y. K.; Chen, Z. W.; Sun, J.; Liu, K.; Chen, W.; Shi, W.; Wang, H. M.; Liu, Y. *J. Org. Chem.* **2002**, *67*, 7624.

(10) Chalier, F.; Tordo, P. *J. Chem. Soc., Perkin Trans. 2* **2002**, 2110.

(11) Villamena, F. A.; Rockenbauer, A.; Gallucci, J.; Velayutham, M.; Hadad, C. M.; Zweier, J. L. *J. Org. Chem.* **2004**, *69*, 7994.

(12) Villamena, F. A.; Hadad, C. M.; Zweier, J. L. *J. Phys. Chem. A* **2003**, *107*, 4407.

(13) (a) Villamena, F. A.; Hadad, C. M.; Zweier, J. L. *J. Am. Chem. Soc.* **2004**, *126*, 1816. (b) Rosen, G. M.; Beselman, A.; Tsai, P.; Pou, S.; Mailer, C.; Ichikama, K.; Robinson, B. H.; Nielsen, R.; Halpern, H. J.; Mackerell, A. D. *J. Org. Chem.* **2004**, *69*, 1321. (c) Clément, J. L.; Ferré, N.; Siri, D.; Karoui, H.; Rockenbauer, A.; Tordo, P. *J. Org. Chem.* **2004**, *69*, 1198. (d) Villamena, F. A.; Hadad, C. M.; Zweier, J. L. *J. Phys. Chem. A* **2005**, *109*, 1662. (e) Villamena, F. A.; Merle, J. K.; Hadad, C. M.; Zweier, J. L. *J. Phys. Chem. A* **2005**, *109*, 6083. (f) Villamena, F. A.; Merle, J. K.; Hadad, C. M.; Zweier, J. L. *J. Phys. Chem. A* **2005**, *109*, 6089.

(14) Petrov, K. A.; Chazov, V. A.; Pastukhova, L. V.; Bogdanov, N. *N. Zh. Obshch. Khim.* **1976**, *46*, 1246.

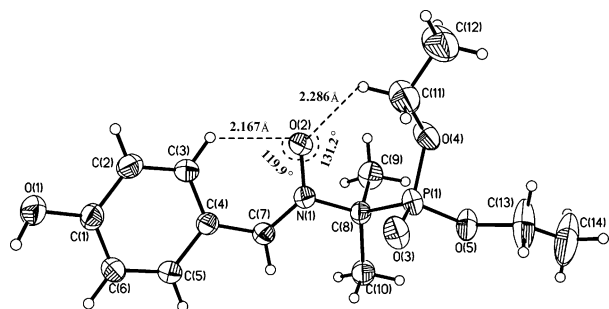


FIGURE 1. ORTEP view of X-ray structure of 4-HOPPN. Broken lines indicate sites of intramolecular hydrogen bonds, and their distances and angles are also given.

structural information for the phosphorylated analogues of PBN. The X-ray crystallographic structure is illustrated in Figures 1, and the corresponding structural details are listed in the Supporting Information as Table S1–S7. It can be seen from Figure 1 that 4-HOPPN contains two intramolecular H-bonds of C(3)–H(3)···O(2) (2.167 Å; 119.9°) and C(11)–H(11a)···O(2) (2.286 Å; 131.2°). Given that there exists only one intramolecular H-bond (2.180 Å; 119.9°) in a crystal of PBN¹⁵ and no H-bond in a crystal of phosphorylated cyclic nitron, DEPPEO,⁹ the presence of two intramolecular H-bonds is probably a special characteristic of the β -phosphorylated analogues of PBN. Additionally, an intermolecular H-bond of O(1)–H(1)···O(3) (1.860 Å; 174.4°) between two adjacent 4-HOPPN is also observed in Table S6 (Supporting Information). Since PPN exists as a viscous oil at room temperature,^{8b} the intermolecular H-bond might be one of the important factors to solidify 4-HOPPN. Analysis of the bond lengths on the nitronyl group indicates that, as shown in Table S3 (Supporting Information), the phosphorylated 4-HOPPN has the shorter N=C bond distance of 1.302(3) Å relative to PBN (1.330(12) Å).¹⁵ Further examination of the X-ray structure suggests that when the spin-trapping reaction occurs, due to the steric blocking effect of the bulky phosphoryl group on C8, attacking radicals should prefer to approach the opposite position relative to the phosphoryl group.

Spin Trapping

(i) Spin Trapping of Superoxide Radical with 4-HOPPN.

When superoxide radical was produced using the light–riboflavin–DTPA superoxide-generating system in the presence of 4-HOPPN, an overlapped ESR spectrum, shown in Figure 2A, was observed. The main signal (▼) is composed of 12-line peaks attributable to a nitroxide that could be suppressed upon the addition of SOD, and therefore, it is assigned to a superoxide spin adduct of 4-HOPPN (4-HOPPN-OOH). Like PPN-OOH,^{5d,8} 4-HOPPN-OOH affords the relatively small α_{H} (Table 1). Besides the superoxide spin adduct, there are also two additional weak signals that are attributed to one signal (●) derived from the electron donor (DTPA)¹⁶ and one three-line signal (*) resulting from a decomposition product of 4-HOPPN, respectively.^{5d,8} However, these paramagnetic species do not limit the use of 4-HOPPN in spin trapping of the superoxide radical, since they do not interfere with the ESR signal of the superoxide spin adduct. The pure signal corresponding to 4-HOPPN-OOH could

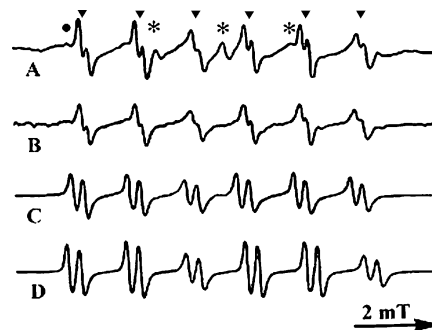


FIGURE 2. Representative ESR spectra of the spin adducts of 4-HOPPN: (A) the superoxide spin adduct (▼) generated by UV irradiation of the aqueous solution containing 4-HOPPN (45 mM), riboflavin (0.1 mM), and DTPA (1 mM), (●), the signal derived from the electron donor (DTPA), (*) the three-line signal resulting from a decomposition product of 4-HOPPN; (B) the superoxide spin adduct produced by addition of H₂O₂ (1%) to 4-HOPPN (50 mM) in pyridine; (C) the CH₃O spin adduct generated by adding a small amount of Pb(OAc)₄ to a solution of 4-HOPPN (50 mM) and methanol (5 M) in DMSO; (D) the *p*-ClPh[•] spin adduct obtained by UV photolysis of a small amount of para-chlorophenyl diazonium tetrafluoroborate in the presence of 4-HOPPN (50 mM) in DMSO. Spectrometer settings: microwave power = 12.9 mW; modulation frequency = 100 kHz; modulation amplitude = 0.03 mT; time constant = 0.33 s; sweep time = 163 s; sweep width = 12 mT.

be obtained by nucleophilic addition of H₂O₂ to 4-HOPPN in pyridine, followed by oxidation of the subsequent hydroxylamine (Figure 2B). As previously observed for the superoxide spin adducts obtained with other nitrones,¹⁷ the lifetime of 4-HOPPN-OOH is significantly longer in pyridine, lasting more than 20 h at room temperature.

The above results allow us to conclude that 4-HOPPN can be used to detect superoxide radical. As a spin trap for superoxide radical, like PPN, one advantage of 4-HOPPN over the commonly used nitrones, such as DMPO, EMPO, and DEPPO, is that it is a solid such that its ease of purification makes 4-HOPPN less susceptible to contamination from paramagnetic impurities.

(ii) Spin Trapping of Other Oxygen-, Carbon-, and Sulfur-Centered Radicals with 4-HOPPN. To further evaluate the potential of 4-HOPPN in the detection of short-lived radicals, a series of oxygen-, carbon-, and sulfur-centered radicals were generated and trapped in DMSO or aqueous solutions. Table 1 lists a summary of all the observed ESR spectral parameters. Whatever the spin adduct considered, the ESR spectrum recorded always consists of 12 lines, due to hyperfine splitting constants (hfsc) with a nitrogen ($I_{\text{N}-14} = 1$), a β -hydrogen ($I_{\text{H}-1} = 1/2$), and a large phosphorus coupling ($I_{\text{P}-31} = 1/2$). Owing to the presence of the additional phosphorus coupling, these spin adducts give more information as compared with that of PBN.

As reported previously, a nucleophilic addition of the alcohol to the nitron, assisted by Pb(OAc)₄, could occur followed by a rapid oxidation of the hydroxylamine to the corresponding alkoxy spin adduct.^{9,18} In the present study, when a large excess of methanol (7.4 M) was added to a solution of 4-HOPPN in DMSO in the presence of a small amount of Pb(OAc)₄, a pure

(17) (a) Reszka, K.; Bilski, P.; Chignell, C. F. *Free Radical Res. Commun.* **1992**, *17*, 377. (b) Tuccio, B.; Lauricella, R.; Fréjaville, C.; Bouteiller, J. C.; Tordo, P. *J. Chem. Soc., Perkin Trans. 2* **1995**, 295.

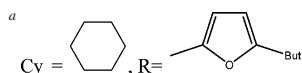
(18) Karoui, H.; Nsanzumuhire, C.; Le Moigne, F.; Tordo, P. *J. Org. Chem.* **1999**, *64*, 1471.

(15) Liu, Y.; Wang, X.; Chen, B.; Xu, G. *J. Struct. Chem.* **1987**, *6*, 17.

(16) Finkelstein, E.; Rosen, G. M.; Rauckman, E. J. *J. Am. Chem. Soc.* **1980**, *102*, 4994.

TABLE 1. ESR Hyperfine Splitting Constants of 4-HOPPN Spin Adducts^a

adduct	source	solvent	α_p (mT)	α_N (mT)	α_H (mT)
HOO•	H ₂ O ₂ riboflavin/hv	pyridine water	3.86 3.88	1.31 1.32	0.16 0.18
CH ₃ O•	CH ₃ OH/Pb(OAc) ₄	DMSO	3.89	1.34	0.28
C ₂ H ₅ O•	C ₂ H ₅ OH/Pb(OAc) ₄	DMSO	3.89	1.34	0.29
<i>n</i> -C ₄ H ₉ O•	<i>n</i> -C ₄ H ₉ OH/Pb(OAc) ₄	DMSO	3.91	1.33	0.27
<i>t</i> -BuO•	(<i>t</i> -BuO) ₂ /hv	DMSO	3.88	1.31	0.28
C ₂ H ₅ S•	C ₂ H ₅ I/hv	DMSO	3.89	1.33	0.21
<i>i</i> -Bu•	<i>i</i> -Bu(O)COSnCy ₃ /hv	DMSO	3.90	1.33	0.26
Ph•	Ph(O)COSnCy ₃ /hv	DMSO	3.91	1.34	0.28
<i>m</i> -BrPh•	<i>m</i> -BrPh(O)COSnCy ₃ /hv	DMSO	3.93	1.34	0.28
<i>m</i> -ClPh•	<i>m</i> -ClPh(O)COSnCy ₃ /hv	DMSO	3.92	1.34	0.28
<i>m</i> -FPh•	<i>m</i> -FPh(O)COSnCy ₃ /hv	DMSO	3.93	1.34	0.27
2,4,6-tri-ClPhOCH ₂ •	(2,4,6-tri-ClPhOCH ₂)(O)COSnCy ₃ /hv	DMSO	3.93	1.34	0.28
R•	R(O)COSnCy ₃ /hv	DMSO	3.92	1.34	0.27
<i>p</i> -IPh•	<i>p</i> -IPh(O)COSnCy ₃ /hv	DMSO	3.89	1.31	0.26
<i>p</i> -MePh•	<i>p</i> -MePh(O)COSnCy ₃ /hv	DMSO	3.91	1.34	0.28
<i>p</i> -NO ₂ PhO•	<i>p</i> -NO ₂ PhOSnCy ₃ /hv	DMSO	3.90	1.32	0.27
PhCH ₂ S•	(PhCH ₂ S) ₂ /hv	DMSO	3.87	1.33	0.27
<i>p</i> -ClPh•	<i>p</i> -ClPhN ₂ ⁺ BF ₄ ⁻ /hv	DMSO	4.20	1.40	0.29



ESR signal assigned to methoxyl spin adduct was observable (Figure 2C). However, with a smaller amount of methanol (1.2 M), another weak signal was also detected besides the methoxyl spin adduct signal (data not shown). The same results were also observed in the case of the ethoxyl and *n*-butoxyl spin adducts. A most likely explanation is that when only a relatively small amount of the alcohol is present, the nitronyl group in one molecule of 4-HOPPN would react with the phenolic group from another one to yield the hydroxylamine that is subsequently oxidized to the corresponding aminoxyl. Therefore, we suggest that one should be careful to use the method of the nucleophilic addition to produce spin adducts of the nitrones containing the phenolic or hydroxyl group because the side product(s) might occur.

Using the UV photolytic method,⁹ we obtained a variety of the aromatic radical adducts (Table 1). When a solution containing 4-HOPPN and a small amount of *p*-chlorophenyl diazonium tetrafluoroborate was irradiated, the strong ESR signal attributed to the *p*-ClPh• spin adduct was observed (Figure 2D).

Attempts to trap HO• in aqueous media, unfortunately, were never successful regardless of the HO• generator. For example, when the Fenton reaction (H₂O₂/Fe²⁺) was used to generate HO• in the presence of 4-HOPPN, the ESR spectrum observed was too complex to assign the presence of the hydroxyl spin adduct (not shown). This may be closely associated with the competition of the phenolic group with the nitronyl group for HO•, since PPN that does not contain the phenolic group (Chart 1) had been shown to be able to trap HO• in aqueous media.^{5d,8a}

(iii) Kinetics of Decay of Superoxide Spin Adduct. The light-riboflavin-DTPA system was utilized to investigate kinetics of decay of the superoxide spin adduct of 4-HOPPN. The ESR signal of the spin adduct persisted for as long as 35 min, as shown in Figure 3. Peak intensities were normalized and plotted. As mentioned above, the presence of the two minor signals does not interfere with the low field peak. Analysis of data shows that the decay plot of the superoxide spin adduct is well fitted with a pure first-order process. Based on the values from the computer simulation, we could calculate the half-life

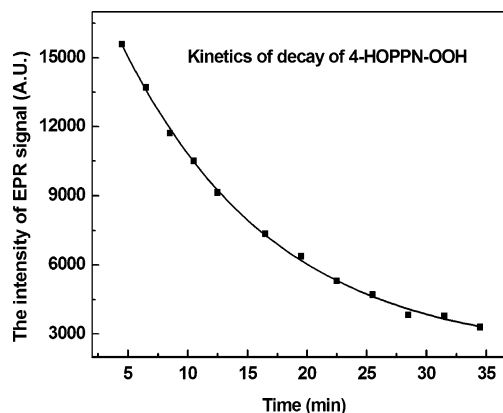


FIGURE 3. Decay plot of the superoxide spin adduct of 4-HOPPN after 1 min of UV irradiation of the aqueous solution containing riboflavin (0.1 mM), 4-HOPPN (45 mM), and DTPA (1 mM).

time ($t_{1/2} \sim 8.8$ min) that was slightly longer than that of the superoxide adduct of PPN.^{8b}

Theoretical Analysis

Optimized Geometries. Selected bond distances for the relevant moieties for the nitronyl spin traps and the respective spin adducts are listed in Table 2 based on the optimized geometries at the B3LYP/6-31G(d) level of theory. As expected, most of the bond distances, including the C–N and N–O bond distances for 4-HOPPN or PBN, are consistent with their X-ray structural data.¹⁵ Meanwhile, the optimized bond distances of three superoxide spin adducts, including C–N, N–O, C–O₂, O–O, and O–H bonds, appear to be comparable to the crystal data from 2,2,5,5-tetramethyl-3-carbamidopyrroline-1-oxyl (TM-CO)¹⁹ and 3,4,4a,5,6,7,8,8a-octahydro-8a-hydroperoxy-2-quinolone,²⁰ respectively.

Thermodynamics of Spin Trapping of Superoxide Radical. The pK_a values for various alkyl hydroperoxides (R-OOH) that

(19) Turley, J. W.; Boer, F. P. *Acta Crystallogr.* **1972**, *B28*, 1641.

(20) Alini, S.; Citterio, A.; Farina, A.; Fochi, M. C.; Malpezzi, L. *Acta Crystallogr.* **1998**, *C54*, 1000.

TABLE 2. Comparison of Selected X-ray Crystallographic Bond Lengths with Calculated Bond Lengths at the B3LYP/6-31G(d) Level of Theory

bonds	bond distance (Å)	
	calcd values	exptl values
C=N	1.31 ^a	1.302(3) ^d
	1.32 ^b	1.330(12) ¹⁵
N-O	1.29 ^a	1.293(3) ^d
	1.27 ^b	1.303(8) ¹⁵
P=O	1.49 ^a	1.4714(19) ^d
P-OR	1.62 ^a	1.5647(19) ^d
	1.61 ^a	1.5608(19) ^d
P-C	1.88 ^a	1.832(2) ^d
C-N	1.48–1.53 ^c	1.50 ²²
N-O	1.29–1.32 ^c	1.27 ²²
C-O ₂	1.39–1.43 ^c	1.441 ²³
O-O	1.43–1.48 ^c	1.4599 ²³
O-H	0.99 ^c	1.02 ²³

^a Calculation from 4-HOPPN. ^b Calculation from PBN. ^c Calculations from their superoxide spin adducts. ^d The crystal data from this work (4-HOPPN).

were experimentally determined to be in the range of 11.65–12.8 are normally smaller than that for water (15.75).^{21,22} Similarly, a recent theoretical study demonstrated that the p*K*_a value for the superoxide spin adduct of DMPO (DMPO-OOH) is about 14.9 ± 0.5.^{13e} Thus, it is the hydroperoxyl form of the spin adduct (4-HOPPN-OOH) rather than its anionic form (4-HOPPN-O₂^{•-}) that mainly exists in the neutral water.

As theoretically proposed, the main species trapped by cyclic DMPO^{13e} or AMPO¹¹ at neutral media was superoxide anionic radical (O₂^{•-}) rather than hydroperoxyl radical (HOO[•]) due to the small p*K*_a value of HOO[•] (approximately 4.8²³ or 4.4²⁴). However, it was experimentally verified that HOO[•] as the acidic form of O₂^{•-} appears to be more reactive than O₂^{•-},^{16,25} which could be further confirmed by the higher reduction potential of HOO[•] (1.06 V) relative to O₂^{•-} (0.94 V).²⁶ In neutral media, to examine whether the low ratio of HOO[•] is possible to take part in spin trapping of superoxide radicals with a linear 4-HOPPN, we comparatively calculated the thermodynamics of two possible routes in which formation of the hydroperoxyl spin adducts was performed by using HOO[•] or O₂^{•-} as an attack species, respectively, as illustrated in the mechanisms A and B of Scheme 2.

Because all of the spin trapping experiments were performed in the aqueous media, we therefore evaluated the varieties of free energy (Δ*G*), both in spin-trapping reactions and in the decomposition of the O₂^{•-} adducts, using the conductor-like polarizable continuum medium (CPCM) model. The solvation contributions to the Δ*G* values are demonstrated in Tables S9 and S10.

It is worth noting that although mechanisms A and B have different sequences of steps, the overall Δ*G* are the same. Formation of the *cis*- and *trans*-isomers of 4-HOPPN-OOH are

overall endoergic with 6.61 and 14.48 kcal/mol, respectively, indicating that formation of *cis*-isomer is more thermodynamically favored. In the mechanism A, a large endoergic step (step 1) is first involved in the formation of the O₂^{•-} adducts (21.65 kcal/mol for the *cis*-isomer and 29.72 kcal/mol for the *trans*-isomer), and then a subsequent protonation of the anionic adduct (step 2) is high exoergic with Δ*G* values of −15.04 kcal/mol for the *cis*-isomer and −15.24 kcal/mol for the *trans*-isomer. Comparatively, Δ*G* value of the formation of HOO[•] (step 3) in mechanism B is only endoergic with 6.57 kcal/mol, and the subsequent trapping of HOO[•] (step 4) is slightly endothermic with 0.04 kcal/mol for the formation of *cis*-isomer and 7.91 kcal/mol for the formation of *trans*-isomer. The comparison evidently indicates that mechanism B is more thermodynamically favorable for both isomers, *cis*-4-HOPPN-OOH and *trans*-4-HOPPN-OOH, than mechanism A. Our result on 4-HOPPN appears to be distinct from the mechanisms of spin trapping of superoxide radical by the cyclic nitrones such as DMPO^{13e} and AMPO¹¹ in which a direct addition of O₂^{•-} to the nitrones (like mechanism A) is more thermodynamically favorable than the addition of HOO[•] (like mechanism B). That two kinds of nitrones (linear and cyclic) bear two distinct reaction mechanisms is associated with the difference of their reactivity for superoxide radical, resulting from their structural discrepancy.²⁷ Once the spin-trapping reaction occurs, the π-system conjugation formed between a benzene ring and a nitronyl group in a linear PBN analogue, 4-HOPPN, would be diminished. Thus, it appears that more energy is required for the linear nitrones in their spin-trapping reactions. For example, the dihedral angle for ∠C4–C7–N–O is 179.5° in 4-HOPPN, almost coplanar, but for two isomers of its superoxide spin adduct, *cis*-4-HOPPN-OOH and *trans*-4-HOPPN-OOH, the angles change to 103.5° and 112.1°, respectively. On the other hand, in the cyclic nitrones, spin-trapping reaction leads to the steric decomposition in the five-membered ring associated with the change from a trigonal to a tetrahedral carbon. The above results imply that the cyclic nitrones have a stronger reactivity for superoxide radical than the linear nitrones.

To distinguish the influence of a *p*-hydroxyl group in the 4-HOPPN, we further conducted a calculation on PPN, a pure phosphorylated analogue of PBN. Analysis of the optimized geometry of PPN evidently finds that its main structural feature is almost as same as that in 4-HOPPN, as listed in Table S8 (Supporting Information). For example, the C=N distance for 4-HOPPN (1.314 Å) is nearly identical with that for PPN (1.314 Å) and as for the N–O bond distance they have similar values (1.290 Å for 4-HOPPN and 1.286 Å for PPN). Consequently, it can be predicted that both 4-HOPPN and PPN have comparable reactivity to trap superoxide radical, and this allows us to evaluate an effect of phosphoryl group in the linear nitrones on the spin trapping reactivity by a comparison between 4-HOPPN and PBN.

In contrast to 4-HOPPN-OOH, the superoxide spin adduct of PBN (PBN-OOH) only provides one isomer due to the absence of the phosphoryl group. On the basis of the most preferred conformation of PBN and its corresponding reaction products, we have likewise calculated two mechanisms (mechanisms A and B) of the formation of PBN-OOH (Table 3). It is clear that mechanism B is thermodynamically preferred for the formation of PBN-OOH, which is the same as that of 4-HOPPN-

(21) Richardson, W. H.; Hodge, V. F. *J. Org. Chem.* **1970**, *35*, 4012.

(22) Gordon, A. J.; Ford, R. A., Eds. *The Chemist's Companion: A Handbook of Practical Data, Techniques, and References*; Wiley-Interscience: New York, 1972.

(23) Behar, D.; Czapski, G.; Rabani, J.; Dorfman, L. M.; Schwarz, H. A. *J. Phys. Chem.* **1970**, *74*, 3209.

(24) Czapski, G.; Bielski, B. H. *J. Phys. Chem.* **1967**, *67*, 2180.

(25) (a) Tsai, P.; Elas, M.; Parasca, A. D.; Barth, E. D.; Mailer, C.; Halpern, H. J.; Rosen, G. M. *J. Chem. Soc., Perkin Trans. 2* **2001**, 875. (b) Tsai, P.; Ichikama, K.; Mailer, C.; Pou, S.; Halpern, H. J.; Robinson, S. H.; Nielsen, R.; Rosen, G. M. *J. Org. Chem.* **2003**, *68*, 7811.

(26) Buettner, G. R. *Arch. Biochem. Biophys.* **1993**, *300*, 535.

(27) Lauricella, R.; Allouch, A.; Roubaud, V.; Bouteiller, J. C.; Tuccio, B. *Org. Biomol. Chem.* **2004**, *2*, 1304.

SCHEME 2. Possible Mechanisms for the Formation of 4-HOPPN-OOH with Free Energies of Reaction (kcal/mol) at the CPCM-B3LYP/6-31+G(d,p)//B3LYP/6-31G(d) Level

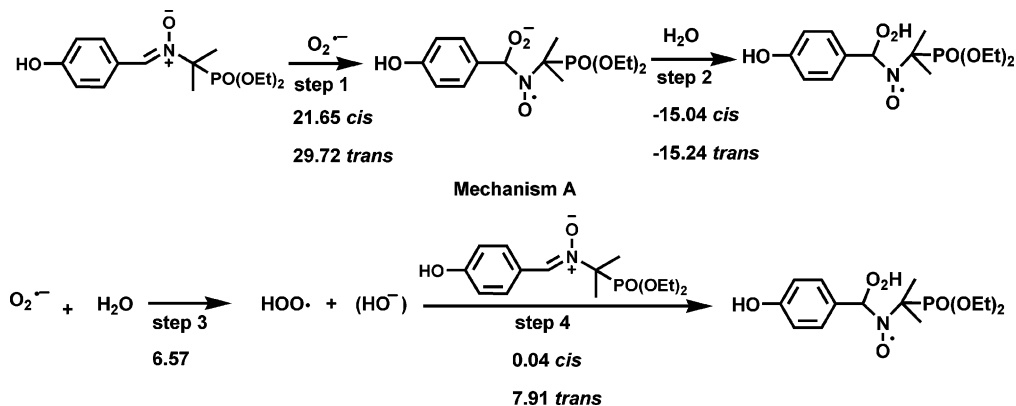


TABLE 3. Reaction Free Energies (kcal/mol) of Various Routes for the Formation of 4-HOPPN-OOH and PBN-OOH at the CPCM-B3LYP/6-31+G(d,p)//B3LYP/6-31G(d) Level

reaction scheme	4-HOPPN-OOH	PBN-OOH
mechanism A		
step 1	21.65 (cis) 29.72 (trans)	25.36
step 2	-15.24 (cis) -16.52 (trans)	-20.86
mechanism B		
step 3	6.57	6.57
step 4	0.04 (cis) 7.91 (trans)	-2.07

OOH. An overall variation of free energy in the spin trapping of superoxide radical by PBN is 4.50 kcal/mol, which indicates that formation of *cis*-4-HOPPN-OOH ($\Delta G = 6.61$ kcal/mol) is almost as feasible as that of PBN-OOH, but *trans*-4-HOPPN-OOH does not ($\Delta G = 14.48$ kcal/mol). Therefore, PBN nearly has an identical thermodynamic tendency of spin trapping of superoxide radical as compared with 4-HOPPN. In other words, an introduction of the phosphoryl group seems not to influence its thermodynamic tendency.

Structural Stability of the Superoxide Spin Adducts. It can be experimentally determined that 4-HOPPN-OOH ($t_{1/2} \sim 8.8$ min) has a similar half-life time with PPN-OOH ($t_{1/2} \sim 6$ min)^{5a,d} in aqueous media, which indicates that an introduction of the hydroxyl group has no obvious effect on the stability of these phosphorylated spin adducts. On the other hand, the half-life time of PBN-OOH could not be determined because of the very fast decay of the spin adduct.² These observations imply that the phosphoryl group may play an important role in stabilizing superoxide spin adducts. Since the introduction of the first cyclic phosphorylated spin trap DEPMPO, many efforts have been made toward uncovering the role of the phosphoryl group. Tordo et al.²⁸ suggested that the strong electron-withdrawing effect and the large steric hindrance of the phosphoryl group were responsible for the stabilities of the linear and cyclic nitronium spin adducts. More recent theoretical data^{13a,d} also revealed that the intramolecular H-bond played an important role in the stability of the superoxide and hydroxyl spin adducts of DEPMPO. However, our previous X-ray structural data⁹ predicted that besides the steric exclusion and the electron-withdrawing effect, the microenvironment around the OOH group also was a significant contributing factor to stabilize the super-

oxide spin adduct of cyclic DEPMPO. With a goal of further clarifying the stabilizing role of the superoxide spin adduct provided by the phosphoryl group of linear nitronium, we comparatively analyzed the optimized geometries of 4-HOPPN-OOH and PBN-OOH.

(i) Intramolecular H-Bond. Two optimized configurations, i.e., *cis*- and *trans*-isomers, are assigned for 4-HOPPN-OOH indicating the position of the diethoxyphosphoryl group relative to the HOO group (Figure 4). Analysis of the optimized *cis* and *trans* isomeric structures reveals that while one strong intramolecular H-bond involving $-P-O \cdots HOO-$ (1.785 Å) is formed in the *cis*-isomer, the *trans*-isomer affords two intramolecular H-bonds involving $-N-O \cdots HOO-$ (2.038 Å) and $-P-O \cdots H-C(7)$ (2.328 Å). According to the optimized geometry of PBN-OOH, we can find a weak H-bond (2.147 Å) on a $-N-O \cdots HOO-$ bond motif as a consequence of the absence of the phosphoryl group. This indicates that the presence of the relatively stronger H-bonds in two isomers of 4-HOPPN-OOH, to some extent, accounts for its higher stability as compared with PBN-OOH. Therefore, we could predict that the phosphoryl group may play a significant role in stabilization of the superoxide spin adduct partly through participation in the formation of the strong intramolecular H-bond. This is in accord with a previous proposal in which the intramolecular H-bond is formed in the superoxide spin adduct of the phosphorylated cyclic nitronium DEPMPO and significantly stabilizes its molecular structure.^{13d}

(ii) Intramolecular Nonbonding Interaction. Besides the intramolecular H-bond, interestingly, there exist many intramolecular nonbonding attractive interactions between the O atom and the neighboring H atom by observations of the optimized geometries of *cis*- and *trans*-4-HOPPN-OOH (Figure 4). All of the distances between the O atom and the neighboring H that vary from 2.464 to 2.946 Å are listed in Table 4 and are totally within the range of nonbonding interaction as previously demonstrated by Tsuzuki (from 2.591 to 2.963 Å).²⁹ Some nonbonding attractive interactions are also present in the optimized geometry of PBN-OOH (Table 4), but when compared with two isomers of 4-HOPPN-OOH, the interactions are evidently weaker due to the absence of the phosphoryl group. As a result, the intramolecular nonbonding attractive interaction involving the O atoms and the H atoms of the phosphoryl group can be expected to be another contributing factor toward the increased stability of 4-HOPPN-OOH.

(28) Tordo, P. *Electron Paramagn. Reson.* **1998**, *16*, 116.

(29) Tsuzuki, S.; Uchimaru, T.; Tanabe, K.; Hirano, T. *J. Phys. Chem.* **1993**, *97*, 1346.

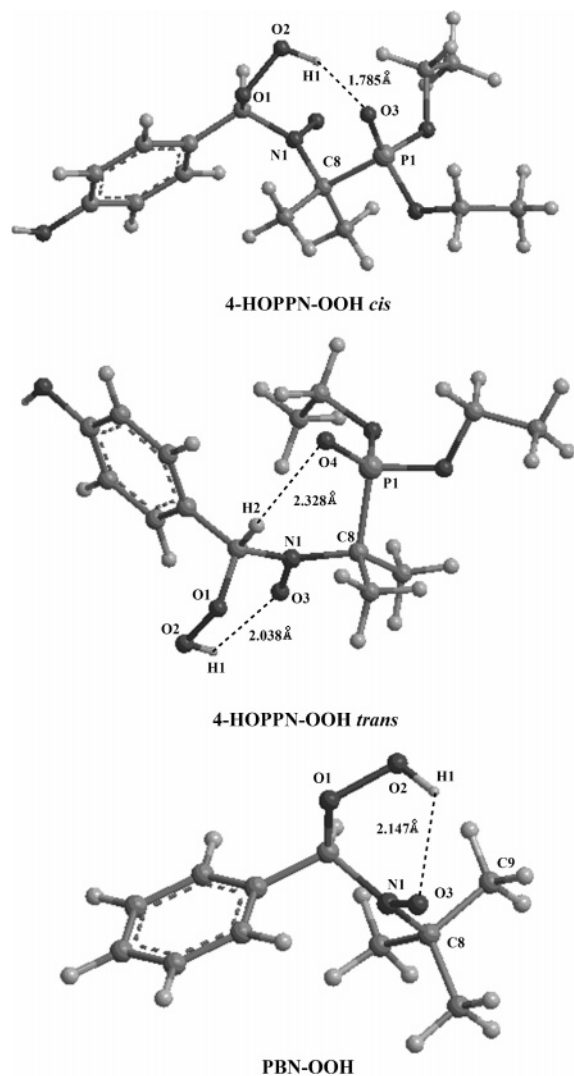


FIGURE 4. 4-HOPPN-OOH (*cis*), 4-HOPPN-OOH (*trans*), and PBN-OOH in optimized structures at the B3LYP/6-31G(d) level of theory. Broken lines indicate sites of intramolecular hydrogen bond, and their distances are also given.

TABLE 4. Selected Nonbonding Distances (Å) and Bond Angles (deg) in the Optimized Geometries of *cis*-4-HOPPN-OOH, *trans*-4-HOPPN-OOH, and PBN-OOH at the B3LYP/6-31G(d) Level of Theory

<i>cis</i> -4-HOPPN-OOH	O (2)–H(5)	2.701	O(3)–H(10a)	2.946
	O (2)–H(9a)	2.464	O(4)–H(9a)	2.787
	O (2)–H(11a)	2.605	O(5)–H(9b)	2.621
	O (2)–H(12a)	2.858	O(5)–H(10b)	2.697
	N(1)–C(8)–P(1)	106.5		
<i>trans</i> -4-HOPPN-OOH	O (2)–H(2)	2.492	O(3)–H(11a)	2.568
	O (2)–H(9a)	2.643	O(3)–H(13a)	2.800
	O (2)–H(9b)	2.531	O(4)–H(9a)	2.706
	O (2)–H(12a)	2.945	O(5)–H(9c)	2.644
	O (3)–H(5)	2.849	O(5)–H(10a)	2.720
N(1)–C(8)–P(1)	106.5			
PBN-OOH	O (1)–H(2)	2.697	O(1)–H(11a)	2.728
	O (1)–H(10a)	2.452		
	N(1)–C(8)–C(9)	107.7		

(iii) **Steric Protection via the Phosphoryl Group.** Steric protection via bulky groups on the adjacent ring carbons (usually methyl groups but sometimes other alkyl groups) has been long considered as one of the most important factors for stabilizing

nitroxide radicals.³⁰ Recently, in the attempts to develop better spin traps for the superoxide radicals, Nohl et al. found that the steric shielding of the spin-bearing nitroxyl group and the peroxy group was a crucial factor that governs stability of the EMPO-derived superoxide spin adducts.³¹ Therefore, it is conceivable that a similar steric effect may exist in 4-HOPPN-OOH. As can be seen from Figure 4, the phosphoryl substituent in the *cis*-HOPPN-OOH is held in close proximity to the hydroperoxy and nitroxyl groups through an intramolecular H-bond and some nonbonding attractive interactions. The steric proximity can be evidently demonstrated by comparison of some spatial angles around C(8); i.e., the angle of N(1)–C(8)–P(1) (106.5°) is smaller than the usual bond angle of sp³ hybrid orbital (109.5°). It can be thus predicted that the large phosphoryl group would contribute to a steric protection of two vulnerable groups, –OOH and nitroxyl, thereby preventing or inhibiting the attack from other molecules (i.e., water) in the solution and, consequently, stabilizing the superoxide adduct. Similarly, in the optimized geometry of *trans*-4-HOPPN-OOH, the H-bond (2.328 Å) involving –P=O···H(7) and some nonbonding attractive interactions (Table 4) also provide a steric protection of the phosphoryl group on the hydroperoxy and the nitroxide moiety (the angle of N(1)–C(8)–P(1) is 106.5°). Comparatively, the steric protection provided by a methyl group in PBN-OOH is much weaker in contrast to the phosphoryl group since the steric proximity of the methyl group (the corresponding angle for N(1)–C(8)–C(9) is 107.7°) to the nitroxyl group and the –OOH is relatively weaker due to the absence of H-bond and weaker nonbonding attractive interactions, as well as its relatively less bulkiness than the phosphoryl group. As a result, the steric protection via a bulky phosphoryl group seems to be another important factor for increasing the stability of 4-HOPPN-OOH.

Thermodynamics of the Decomposition of the Superoxide Adducts. Although the exhaustive elucidation of the decay mechanisms of the nitron radical adducts, especially their superoxide spin adducts, is valuable in the development of better spin traps, its theoretical study has not received much attention. Until recently, only one study using DFT theory has shed light on the thermodynamics of decay of DMPO-OOH and DEP-MPO-OOH.^{13f} To give further insight into the stability of 4-HOPPN-OOH and to provide new clues for stabilizing some other linear or cyclic superoxide spin adducts, we herein conducted theoretical calculation on the thermodynamics of the 4-HOPPN-OOH decay.

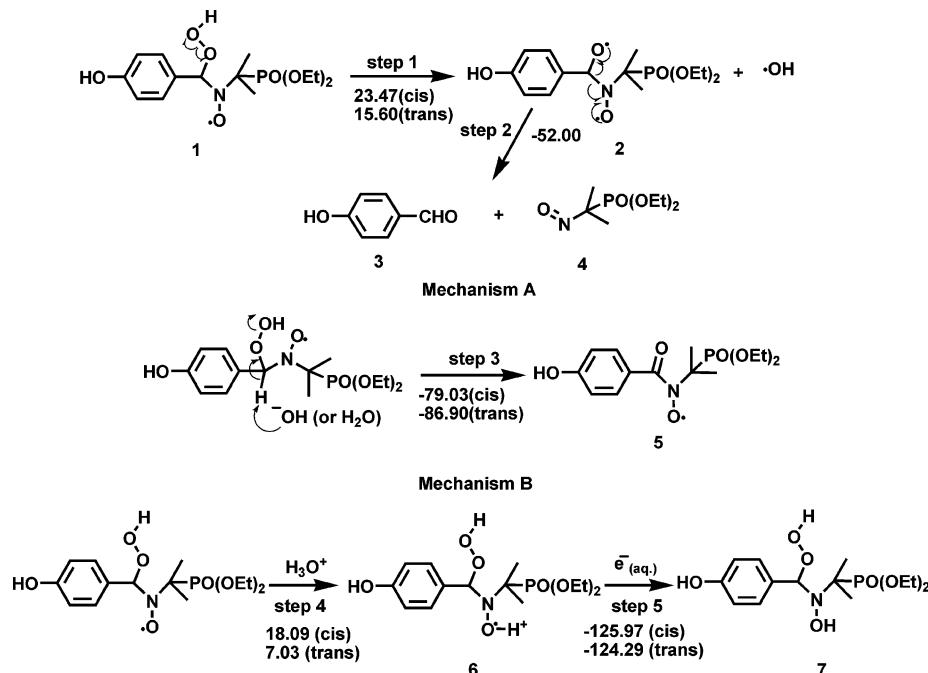
As experimentally observed,^{17b} decay of the nitron superoxide spin adducts usually included first- or second-order kinetic process. However, the experimental ESR observation discussed above has indicated that only first-order kinetics occurs during the 4-HOPPN-OOH decay (Figure 2), which is consistent with the decays of PPN-OOH and 4-PyOPN-OOH.^{8b} Therefore, the following section focuses mainly on the unimolecular decay of 4-HOPPN-OOH.

Although the actual first-order decay mechanism of the superoxide spin adducts produced from the phosphorylated linear nitrones have not received much attention, there is some indirect evidence that could aid in elucidating the relevant reaction type.

(30) Kocherginsky, N.; Swartz, H. M. *Nitroxide Spin Labels. Reaction in Biology and Chemistry*; CRC Press: Boca Raton, New York, London, Tokyo, 1995; p 27.

(31) (a) Stolze, K.; Udilova, N.; Rosenau, T.; Hofinger, A.; Nohl, H. *Biol. Chem.* **2003**, *384*, 493. (b) Stolze, K.; Udilova, N.; Rosenau, T.; Hofinger, A.; Nohl, H. *Biochem. Pharmacol.* **2003**, *66*, 1717.

SCHEME 3. Possible Mechanism of Various Decomposition Pathways of 4-HOPPN-OOH and PBN-OOH with Free Energies of Reaction (kcal/mol) at the CPCM-B3LYP/6-31+G(d,p)//B3LYP/6-31G(d) Level



For instance, Kotake and Janzen³² previously proposed that a unimolecular reaction involving the C–N bond cleavage might occur during the decay of the hydroxyl adduct of PBN. Other evidence of this cleavage could be provided by analysis of the decomposition products of the hydroxyl spin adduct of the linear phosphorylated³³ and esterated³⁴ nitrones. More recent theoretical studies further demonstrated that the C–N bond-breaking process played a crucial role in the stability of hydroxyl^{13a} and superoxide^{13f} spin adducts for cyclic nitrones. Similarly, the C–N bond-breaking process is probably involved in the unimolecular decay of 4-HOPPN-OOH, a superoxide spin adduct obtained from linear 4-HOPPN. On the other hand, a previous study³⁵ found that the peroxy spin adducts of PBN underwent decomposition via the C–H^β bond cleavage, generating bezoyl *tert*-butyl nitroxide. The nitroxyl ketone was also observable during the decomposition of PBN-OOH in the presence of cyclodextrins.³⁶ Further evidence revealed that the cleavage might be labile during the decomposition of DMPO-OOH.³⁷ Hence, the C–H^β bond cleavage should be considered during the decay of the superoxide spin adduct; In addition, the reduction of nitroxide to hydroxylamine took place when both an electron and a H⁺ donor were present in the solution.³⁰

The reduction route was much more labile in the biological systems containing sulfhydryl reagents,³⁸ ascorbic acid,³⁹ mitochondrial electron transport chain,⁴⁰ cytochrome *P*-450,⁴¹ and bacterial electron transport systems.⁴²

On the basis of the above analysis, we separately analyzed the three possible routes for the unimolecular decomposition of 4-HOPPN-OOH, as illustrated in Scheme 3. In the decay process involving C–N bond cleavage (mechanism A), 4-HOPPN-OOH decomposes through two steps. The homolytic cleavage of the hydroperoxyl O–O bond⁴³ (step 1) produces a diradical intermediate 2 (in triplet or singlet) and a hydroxyl radical, and then the diradical 2 undergoes a C–N bond cleavage to yield a nitroso 3 and a 4-hydroxybenzaldehyde 4 (step 2). Attempts to locate the singlet structure of 2 suffered from failure, but 3 and 4 were ultimately obtained through the triplet. Although formation of the diradical 2 (in triplet) is endoergic with the ΔG value of 23.47 kcal/mol (*cis*-isomer) and 15.60 kcal/mol (*trans*-isomer), subsequently, conversion of 2 to the nitroso and the aldehyde provides a free energy of –52.00 kcal/mol. As usually observed during the decay of some superoxide spin adducts, the HO· thus generated may be trapped by the nitrone to form a hydroxyl spin adduct.^{10,34a,44} Nevertheless, the hydroxyl spin adduct of 4-HOPPN has not been experimentally observed, possibly due to a H-abstraction from 4-HOPPN by

(32) Kotake, Y.; Janzen, E. G. *J. Am. Chem. Soc.* **1991**, *113*, 9503.

(33) (a) Rizzi, C.; Lauricella, R.; Tuccio, B.; Bouteiller, J. C.; Cerri, V.; Tordo, P. *J. Chem. Soc., Perkin Trans. 2* **1997**, 2507. (b) Allouch, A.; Roubaud, V.; Lauricella, R.; Bouteiller, J. C.; Tuccio, B. *Org. Biomol. Chem.* **2003**, *1*, 593. (c) Janzen, E. G.; Kotake, Y.; Hinton, R. *Free Radic. Biol. Med.* **1992**, *12*, 169. (d) Janzen, E. G.; Hinton, R.; Kotake, Y. *Tetrahedron Lett.* **1992**, *33*, 1257.

(34) Roubaud, V.; Lauricella, R.; Bouteiller, J. C.; Tuccio, B. *Arch. Biochem. Biophys.* **2002**, *397*, 51.

(35) Niki, E.; Yokoi, S.; Tsuchiya, J.; Kamiya, Y. *J. Am. Chem. Soc.* **1983**, *105*, 1498.

(36) Karoui, H.; Tordo, P. *Tetrahedron Lett.* **2004**, *45*, 1043.

(37) (a) Finkelstein, E.; Rosen, G. M.; Rauckman, E. J.; Paxton, J. *Mol. Pharm.* **1979**, *16*, 676. (b) Briere, R.; Rassat, A. *Tetrahedron* **1976**, *32*, 2891. (c) Villamena, F. A.; Dickman, M. H.; Crist, D. R. *Inorg. Chem.* **1998**, *37*, 1446. (d) Villamena, F. A.; Dickman, M. H.; Crist, D. R. *Inorg. Chem.* **1998**, *37*, 1454.

(38) Gaffney, B. J. *Spin Labeling Theory and Application*; Academic Press: New York, 1976; 183.

(39) Smith, I. C. P. *Biological Applications of Electron Spin Resonance*; Wiley-Interscience: New York, 1972; 483.

(40) Likhtenshtein, G. T. *Spin Labeling Methods in Molecular Biology*; Wiley-Interscience: New York, 1976; p 190.

(41) (a) Stier, A.; Sackman, E. *Biochim. Biophys. Acta* **1973**, *311*, 400. (b) Rosen, G. M.; Rauckman, E. J. *Biochem. Pharmacol.* **1977**, *26*, 675.

(42) Goldberg, J. S.; Rauckman, E. J.; Rosen, G. M. *Biochim. Biophys. Res. Commun.* **1977**, *79*, 198.

(43) Finkelstein, E.; Rosen, G. M.; Rauckman, E. J. *Mol. Pharm.* **1982**, *21*, 262.

(44) Karoui, H.; Clément, J. L.; Rockenbauer, A.; Siri, D.; Tordo, P. *Tetrahedron Lett.* **2004**, *45*, 149.

TABLE 5. Reaction Free Energies (kcal/mol) of Various Decomposition Pathways for 4-HOPPN-OOH and PBN-OOH at the CPCM-B3LYP/6-31+G(d,p)//B3LYP/6-31G(d) Level

reaction scheme	4-HOPPN-OOH	PBN-OOH
mechanism A		
step 1	23.47 (cis) 15.60 (trans)	23.68
step 2	-52.00	-50.53
mechanism B		-79.93
step 3	-79.30 (cis) -86.90 (trans)	
mechanism C		
step 4	18.09 (cis) 7.03 (trans)	8.86
step 5	-125.97 (cis) -124.29 (trans)	-121.98

HO[•], as mentioned within the “spin trapping” in the Experimental Section.

In the decomposition process via C–H^β bond cleavage (mechanism B), possibly induced by HO[•] or H₂O, the C–H^β bond cleavage yields a nitroxyl-ketone **5** through the elimination of a H₂O molecule (step 3). The process is more favorable with Δ*G* values of -79.03 kcal/mol (*cis*-isomer) and -86.90 kcal/mol (*trans*-isomer) relative to the step 1 of mechanism A.

The above theoretical analysis reveals that 4-HOPPN and PBN possess comparable spin-trapping potency for superoxide radical, but spin-trapping ESR experiments prove that only 4-HOPPN superoxide adduct is detectable in aqueous media. To clarify the contradiction, we have to comparatively analyze the decays of both spin adducts, 4-HOPPN-OOH and PBN-OOH. All the free energies in each step of the PBN-OOH decay were thermodynamically calculated using similar three reaction models. As shown in Table 5, it is clear that, both in mechanisms A and B, there is no significant difference in the overall or stepwise energies of decay between *cis*-4-HOPPN-OOH and PBN-OOH. However, a comparison of decay of the *trans*-4-HOPPN-OOH with that of PBN-OOH reveals that the *trans*-isomer appears to be thermodynamically unstable in two possible processes, mechanisms A and B, in which the *trans*-4-HOPPN-OOH decay is 9.55 and 7.17 kcal/mol more exoergic than the PBN-OOH decay, respectively. That is to say, according to the calculations based on two mechanisms, that neither *trans*-4-HOPPN-OOH, nor *cis*-4-HOPPN-OOH, can decay slower than PBN-OOH does. These thermodynamic calculations are obviously contradicted with their ESR observations when comparing the distinct difference between the lifespan of PBN-OOH and 4-HOPPN-OOH, and thus, two mechanisms do not account for the decays. Examination of the formation of the corresponding hydroxylamine (mechanism C) shows that the H⁺-accepting reaction (step 4) for *cis*-4-HOPPN-OOH is more endothermic with Δ*G* of 18.09 kcal/mol as compared to the value of 8.83 kcal/mol for PBN-OOH. The subsequent decay via electron transfer (step 5) is considerably exothermic, and their Δ*G* values are approximately same for *cis*-4-HOPPN-OOH and PBN-OOH. Accordingly, the rate-limiting step is probably the H⁺-accepting reaction (step 4), and in mechanism C, PBN-OOH decay is more thermodynamically favored than 4-HOPPN-OOH decay. Moreover, in the kinetic view, both the protonation process and the subsequent electron transfer for 4-HOPPN-OOH are less favorable due to the large steric protection of the oxygen of the nitroxyl group provided by the bulky phosphoryl group as compared with PBN-OOH. Therefore, mechanism C is a possible pathway that is responsible for the different lifespan

of PBN-OOH and 4-HOPPN-OOH. In fact, hydroxylamines derived from PBN spin adducts were detected in the *in vivo* spin-trapping experiment.⁴²

Conclusions

A new phosphorylated analogue of PBN, 4-HOPPN, has been prepared, and its crystal structure has been determined by the X-ray diffraction. Spin-trapping experiments demonstrate that 4-HOPPN can be used to trap various carbon-, oxygen-, and sulfur-centered radicals. Like other phosphorylated linear nitrones, 4-HOPPN significantly stabilizes its superoxide spin adduct (*t*_{1/2} ~ 8.8 min). To elucidate the role of the phosphoryl group, theoretical calculation using DFT were utilized to investigate the mechanisms of spin trapping of superoxide radical by 4-HOPPN and PBN, as well as to analyze the structural stability and the decay mechanisms of 4-HOPPN-OOH and PBN-OOH. Our calculations show that both 4-HOPPN and PBN share a common mechanism and have, thermodynamically, a comparable potency for spin trapping of superoxide radical. Examination of the optimized geometries of 4-HOPPN-OOH and PBN-OOH reveals that there exist some stronger intramolecular interactions, including the H-bonds and the nonbonding attractive interactions, as well as larger steric protection in 4-HOPPN-OOH, when compared to those in PBN-OOH. All of the intramolecular interactions and the protections are probably responsible for stabilizing the superoxide spin adducts. Finally, the higher stability of 4-HOPPN-OOH has reasonably been verified by comparing its decomposition thermodynamics using three various possible routes.

Experimental Section

Synthesis of *N*-(4-Hydroxybenzylidene)-1-diethoxyphosphoryl-1-methylethylamine *N*-Oxide (4-HOPPN). To a solution of 4-hydroxybenzaldehyde (0.50 g, 4.5 mmol) in anhydrous THF (30 mL) under nitrogen were added diethyl (1-hydroxyamino-1-methylethyl)phosphonate (0.85 g, 4 mmol) and a small amount of dry MgSO₄, and the mixture was stirred for 3 h under reflux. The reaction mixture was filtered and then concentrated *in vacuo* to give a pale yellow solid which was purified by silica gel column chromatography by using a solvent system of dichloromethane and ethanol (30:1) and crystallized from the mixed solvent of *n*-hexane and ethyl acetate. 4-HOPPN was obtained as a colorless crystal (1.01 g, 80.2%). Mp: 138.5–139.5 °C. UV (C₂H₅OH; λ_{max}/nm): 312.5. ¹H NMR (CDCl₃; ppm): δ 1.442 (6H, t), 1.890 (6H, d, *J* = 15.3 Hz), 4.278 (4H, m), 6.787 (2H, d, *J* = 8.7 Hz), 7.408 (H, s), 7.910 (2H, d, *J* = 8.6 Hz). ¹³C NMR (CDCl₃; ppm): δ 15.41, 22.30, 62.92, 71.75, 114.71, 120.85, 130.38, 132.32, 158.70. ³¹P NMR (CDCl₃, H₃PO₄, external standard; ppm): δ 22.87. MS (ESI, *m/z*): 316.2 ([M + H]⁺, 100), 338.2 ([M + Na]⁺, 38.5), 354.1 ([M + K]⁺, 8.2).

Spin Trapping Studies. (a) ESR Measurements. X-band ESR spectra were recorded at room temperature. The spectrometer settings were normally at the modulation amplitude of 0.1 mT, modulation frequency of 100 kHz, microwave power of 12.9 mW, and microwave frequency of 9.5 GHz. UV photolysis was performed by a 200 W high-pressure mercury lamp.

(b) Spin Trapping of Superoxide Radical. The superoxide adduct (4-HOPPN-OOH) was generated using two systems: (a) riboflavin–DTPA–light system, an aqueous solution containing riboflavin (0.1 mM), 4-HOPPN (45 mM) and DTPA (1 mM), illuminated with UV light; (b) a pyridine solution of H₂O₂ (1%) and 4-HOPPN (45 mM).

(c) Spin Trapping of Alkoxy Radicals. The spin adducts of methoxyl, ethoxyl, and *n*-butoxyl radicals were produced by adding

a small amount of $\text{Pb}(\text{OAc})_4$ to a solution of 4-HOPPN (50 mM) and the desired alcohol (7.4 M) in DMSO. *tert*-Butoxyl radical was generated by UV photolysis of a solution of di-*tert*-butyl peroxide (1 M) in the presence of 4-HOPPN (50 mM) in DMSO.

(d) Spin Trapping of Thiol Radical. PhCH_2S was generated by UV photolysis of a solution of dibenzyl disulfide (1.5 M) and 4-HOPPN (50 mM) in DMSO.

(e) Spin Trapping of Other Radicals. Other radicals were generated by UV photolysis of a solution of corresponding sources (1 M) in the presence of 4-HOPPN (50 mM) in DMSO.

(f) Kinetics of Decay of Superoxide Spin Adduct. In a typical decay kinetic study, an aqueous solution containing riboflavin (0.1 mM), 4-HOPPN (45 mM), and DTPA (1 mM) was irradiated for 1 min. The spin adduct decay was followed by monitoring the decrease of the lowest field peak. Computer simulations were performed by use of Origin 7.0. In these calculations, the monitored ESR peak intensity is related to the actual radical concentration by a scale factor.

Computational Methods. Density functional theory (DFT) was applied in this study to determine the optimized geometry, vibrational frequencies, and single-point energy of all stationary points. The elaborate calculation procedures are the following. The molecular geometries were optimized first by molecular mechanic method MMX, and then, by B3LYP functional on basis set of 6-31G(d). All the stable structures without virtual vibrational frequencies were gained. The zero point vibrational energy (ZPVE) and the vibrational contribution to the enthalpy and entropy were scaled by a factor of 0.9806.¹² Finally, the single-point energies were gained using B3LYP/6-31+G(d,p). The solvent effect was also considered by employing the self-consistent reaction field (SCRF) method with conductor-like polarizable continuum medium

(CPCM) model.⁴⁵ All quantum chemical calculations were performed with Gaussian 98.⁴⁶

Structural Determination. Single crystals of 4-HOPPN were produced by recrystallization followed by a crystal-growing process. The recrystallization involved heating the nitron and proper amount of the hexane. Ethyl acetate was then slowly added to the mixture until dissolved. The resulting solution was put into a crystal-growing bottle while still hot. Hexane vapor was used to slowly diffuse into the solution until a perfect crystal was produced. Data for 4-HOPPN was collected on a Rigaku R-axis Rapid IP diffractometer with a graphite monochromator. The structure was solved by direct methods and refined by full-matrix least-squares methods on F^2 . All calculations were performed by SHELX97.⁴⁷ Full details of the crystallographic data for 4-HOPPN are described in the Supporting Information.

Acknowledgment. The investigation was supported by NSFC (No. 20473098) and the Outstanding Overseas Chinese Scholars Fund of Chinese Academy of Sciences (2005-1-12).

Supporting Information Available: X-ray crystallographic data (CIF). Energies, enthalpies, and free energies for the spin traps, their superoxide adducts, and the decomposition products of the superoxide adducts. This material is available free of charge via the Internet at <http://pubs.acs.org>.

JO061204M

(45) Barone, V.; Cossi, M. *J. Phys. Chem. A* **1998**, *102*, 1995.

(46) Frisch, M. J.; Trucks, G. W.; Schlegel, H. B.; et al. *Gaussian 98*, revision A.11; Gaussian, Inc.: Pittsburgh, PA, 2001.

(47) (a) Sheldrick, G. M. *Acta Crystallogr.* **1990**, *A46*, 467. (b) Sheldrick, G. M. Program for the Refinement of Crystal Structures, University of Göttingen.